**D.V.N.Ananth[1],
Dr. G.V. Nagesh
Kumar[2],***

Performance of grid connected DFIG during recurring symmetrical faults using Internal Model Controller based Enhanced Field Oriented Control

The modern grid rules forces DFIG to withstand and operate during single as well as multiple low voltage grid faults. The system must not lose synchronism during any type of fault for a given time period. This withstanding capacity is called low voltage ride through (LVRT). To improve performance during LVRT, enhanced field oriented control (EFOC) method is adopted in rotor side converter. This method helps in improving power transfer capability during steady state and better dynamic and transient stability during abnormal conditions. In this technique, rotor flux reference change from synchronous speed to some smaller speed or zero during the fault for injecting current at the rotor slip frequency. In this process, DC-Offset component of flux is controlled beyond decomposing to a lower value during faults and maintaining it. This offset decomposition of flux will be oscillatory in conventional FOC, whereas in EFOC with internal model controller, flux can damp quickly not only for single fault but during multiple faults. This strategy can regulate stator and rotor current waveform to sinusoidal without distortion during and after fault. It has better damped torque oscillations, control in rotor speed and generator flux during and after fault. The fluctuations in DC bus voltage across capacitor are also controlled using proposed EFOC technique. The system performance with under-voltage grid fault of 30% and 60% of the rated voltage occurring at the point of common coupling during 1 to 1.25 and another fault between 1.6 to 1.85 seconds are analyzed using simulation studies.

Keywords: DFIG; Field oriented control; Internal model control; low voltage ride through; recurring faults; recurring faults.

Article history: Received 14 October 2015, Accepted 8 February 2016.

1. INTRODUCTION

The doubly fed induction generator (DFIG) is proved to have many advantages compared to same class of wind turbine driven generators. It has major advantages like better real and reactive power capability, variable speed constant frequency operation etc. However, it is sensitive to external disturbances like voltage swell and sag if not controlled effectively. The modern strict grid rules suggest DFIG needs to operate effectively for single fault as well as for multiple faults.

The status of research on the low voltage ride through (LVRT) issue for DFIG for symmetrical and asymmetrical faults and comparison of different control strategies is given in [1]. Understanding the capability of rotor side converter (RSC) to deliver desired reactive power and withstanding capability during fault in [2]. LVRT enhancement based on flux trajectory [3], enhanced reactive power support [4], controlling DC link current of RSC to smoothen DC voltage fluctuations due to grid faults by using stored Kinetic Energy [5], crowbar as passive and RSC strategy as active compensation for LVRT Q compensation [6], FFTC scheme with PIR [7] and PI [8] with symmetrical and asymmetrical faults for improving uninterrupted P, Q supply from wind turbine (WT) to grid. Few intelligent control techniques like Genetic Algorithm [9] and bacterial search etc were used for improving the performance during LVRT. The recurring symmetrical and asymmetrical fault analysis and

* Corresponding author: GITAM University, Rushikonda, Visakhapatnam, 530045, Andhra Pradesh, INDIA,
Tel.: +91 9000573759, E-mail address: drgvnk14@gmail.com (G.V. Nagesh Kumar)
[1] Department of EEE, Viswanadha Institute of Technology and Management, Visakhapatnam,531173, India
[2] Department of EEE, GITAM University , Visakhapatnam, 530045, Andhra Pradesh, INDIA, India

the performance of DFIG are studied in [10-15]. The performance of DFIG using robust controllers like PI, dual PI and PIR for asymmetrical and symmetrical faults is done in [16]. Here with PIR, the results like DC link voltage, torque ripples minimized. Overall system performance is improved. With all the above techniques, phase sequence components analysis or rigorous mathematical analysis is required. This makes the system control more complex. Hence there is a need to have a better control strategy for multiple (recurring) faults with enhanced operation during any type of fault.

There are few situations in which faults may not be cleared in single reclosing and is found to occur multiple times. This type of situation is called recurring faults. With new modern grid code demand for wind energy system, the authors in [10-16] studied the behavior of DFIG WT system for single or multiple severe faults at grid. The mitigation of DFIG voltage and current profile are not analyzed clearly.

In general for severe grid faults, there will be large electromagnetic torque (EMT) oscillation, stator terminal voltage to decrease, DC link voltage across capacitor increases and speed of rotor increases. The basic objective of this paper is to minimize all these affects and further to improve the voltage and current profile of stator and rotor during faults. During first grid fault, stator EMF decreases with decrease in the flux value. However, during the second and multiple faults, natural stator flux production depends on dip in stator voltage, recovery from first fault, duration between faults, time constants of stator and rotor winding circuits. The system performance is studied under two cases with 30% and 60% decrease in grid voltage during 1 to 1.25s and 1.6 to 1.85 seconds symmetrical faults occurs near point of common coupling (PCC). The voltage, current and flux parameters at rotor, stator windings, grid voltage and DFIG electromagnetic torque, speed of the rotor were compared and analyzed for the two cases with internal model controller (IMC).

The basic objective of this paper is to minimize all the affects during grid disturbances. It further aims to improve the voltage and current profile of stator and rotor during faults. During phase-A dip or rise in grid voltage, stator EMF decreases with decrease in the flux value. The electromagnetic torque (EMT) oscillations occur during single or two phases dip and reach to very low or zero value. Also, when a fault occurs, due to slower response mechanical energy remains almost constant compared to decrease in electrical energy output. This difference in energy conversion makes rotor shaft to rotate quicker and tends the system towards instability. If decay in rotor flux is controlled, stability can be regained. This can be achieved by controlling the offset component of stator flux by changing its synchronous speed reference to a new reference value. Also control in DC link voltage across capacitor also plays a vital role. Hence EFOC technique is developed to control decay in rotor flux, varying synchronous speed of stator, better reactive power control to limit the deviation in electro-mechanical conversion during faults. Within the scope of its power limits, for any type of sag or swell asymmetrical and symmetrical disturbances, DFIG with EFOC helps in improving reliability and lifetime of overall system. The efficacy of system with sag during recurring faults will be analyzed in the next section.

In the section 2, deign of converters for EFOC is explained. In section number 3, mathematical modeling of wind turbine and generator converters for the grid connected DFIG was explained during transient state. In this section, effect of system during symmetrical fault, EFOC control technique and behavior of mechanical and electrical system with variation in rotor speed is explained in sub-sections. In section 4, proposed IMC is described briefly. Further sections 5 describe the simulation results with voltage sag of 30% and 60% of the rated voltage with IMC is verified using MATLAB environment. The conclusion are given in section 6, appendix and references follows.

2. Design of Rotor Side Converter Control for EFOC

RSC controller helps in improving reactive power demand at grid and to extract maximum power from the machine by making the rotor to run at optimal speed. The optimal speed of the rotor is decided from machine real power and rotor speed characteristic curves from MPPT algorithm. The stator active and reactive power control is possible with the RSC controller strategy through i_{qr} and i_{dr} components controlling respectively. The rotor voltage in a stationary reference frame [6] and further analysis from [17] is given by

$$V_r^s = V_{0r}^s + R_r i_r^s + \sigma L_r \frac{di_r^s}{dt} - j\omega\, i_r^s \tag{1a}$$

with $\sigma = 1 - \frac{L_{sm}^2}{L_s L_r}$ and

ω is the rotor speed, i_r^s is the rotor current in a stationary frame of reference, Ls, Lr and Lm are stator, the rotor and mutual inductance parameters in Henry or in p.u.

$$V_{0r}^s = \frac{L_m}{L_s}(\frac{d}{dt} - j\omega_s)\Phi_s^s \tag{1b}$$

It is the voltage induced in the stator flux. Using basic equations, we can get rotor d and q axis voltages as

$$V_{dr} = (R_r + \frac{dL_r'}{dt})i_{dr} - s\omega_s L_r' i_{qr} + \frac{L_m}{L_s}V_{ds} \tag{2}$$

$$V_{qr} = (R_r + \frac{dL_r'}{dt})i_{qr} + s\omega_s L_r' i_{dr} + \frac{L_m}{L_s}(V_{qs} - \omega\Phi_{ds}) \tag{3}$$

where ω is rotor speed, $\omega_{\Phi s}$ is speed of stator flux, ω_s is synchronous speed.

The above equations 2 and 3 can be rewritten in terms of decoupled parameters and are designed for RSC controller as in equations 4 and 5.

$$\sigma V_{dr} = \sigma L_r \frac{dI_{dr}}{dt} - \omega_s\Phi_{qr} + \frac{L_m}{L_s}(V_{ds} - R_s I_{ds} + \omega_1\Phi_{qs}) \tag{4}$$

$$\sigma V_{qr} = \sigma L_r \frac{dI_{qr}}{dt} + \omega_s\Phi_{dr} - \frac{L_m}{L_s}(R_s I_{qs} + \omega_1\Phi_{ds}) \tag{5}$$

In general the rotor speed ω_r is and the synchronous speed of stator is ω_s .But this synchronous frequency has to be changed from ω_s to a new synchronous speed value as described in flowchart ω_s' [17] as it is represented commonly by ω_1 . Under ideal conditions, reference stator d-axis flux Φ_d^* is zero and q-axis flux Φ_q^* is equal to the magnitude of stator flux Φ_s for given back emf and rotor speed. The transient rotor d-q current is given by equations (6A and 6B) as

$$\frac{di_{dr}}{dt} = \frac{-R_r}{\sigma L_r}i_{dr} + s\omega_s i_{qr} + \frac{1}{\sigma L_r}V_{dr} \tag{6A}$$

$$\frac{di_{qr}}{dt} = \frac{-1}{\sigma}(\frac{R_r}{L_r} + \frac{R_s L_m^2}{L_s^2 L_r})i_{qr} + s\omega_s i_{dr} + \frac{1}{\sigma L_r}V_{qr} \tag{6B}$$

The reference rotor voltages in d-q transformation can be rewritten from equations 4 and 5 and from the control circuit are given below. This is the output voltage from rotor windings during normal and transient conditions.

$$V_{qr}^* = \left(i_{dr}^* + \frac{1}{\sigma}(\frac{R_r}{L_r} + \frac{R_s L_m^2}{L_s^2 L_r})i_{qr} + s\omega_s i_{dr}\right)\sigma L_r \tag{7A}$$

$$V_{qr}^* = \left(i_{dr}^* + \frac{1}{\sigma}(\frac{R_r}{L_r} + \frac{R_s L_m^2}{L_s^2 L_r})i_{qr} + s\omega_s i_{dr}\right)\sigma L_r \tag{7B}$$
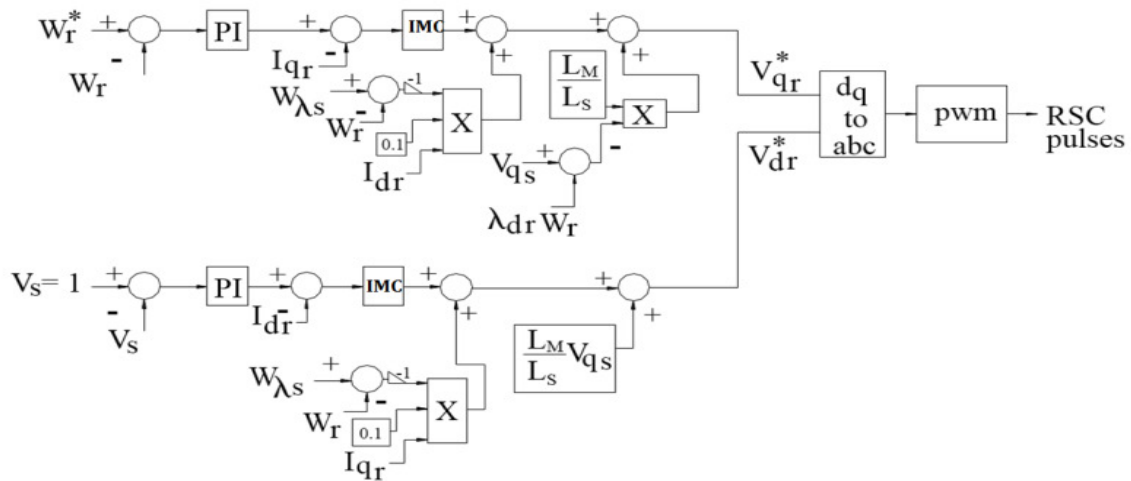
Fig. 1a Complete RSC controller design

The overall block diagram of RSC is presented in Fig. 1a and GSC is shown in Fig. 1b. The rotor speed is multiplied with pole numbers and is subtracted from angular grid synchronous frequency. Later integrated and given a 90o phase shift to get rotor slip injection frequency angles (θs). The flux derivation technique helps in understanding the operation of DFIG during steady state and transient state. The accuracy of system performance during steady state depends on accuracy of wind speed measurement action of pitch angle controller, measurement of stator current, voltage, flux and other parameters. The more accurate these measurements, the more can be real power extracted from DFIG wind turbine system. The equations 4 to 7 play a vital role in understanding the behavior of DFIG during steady state and transients. The accuracy of RSC depends on control of d and q axis voltages.
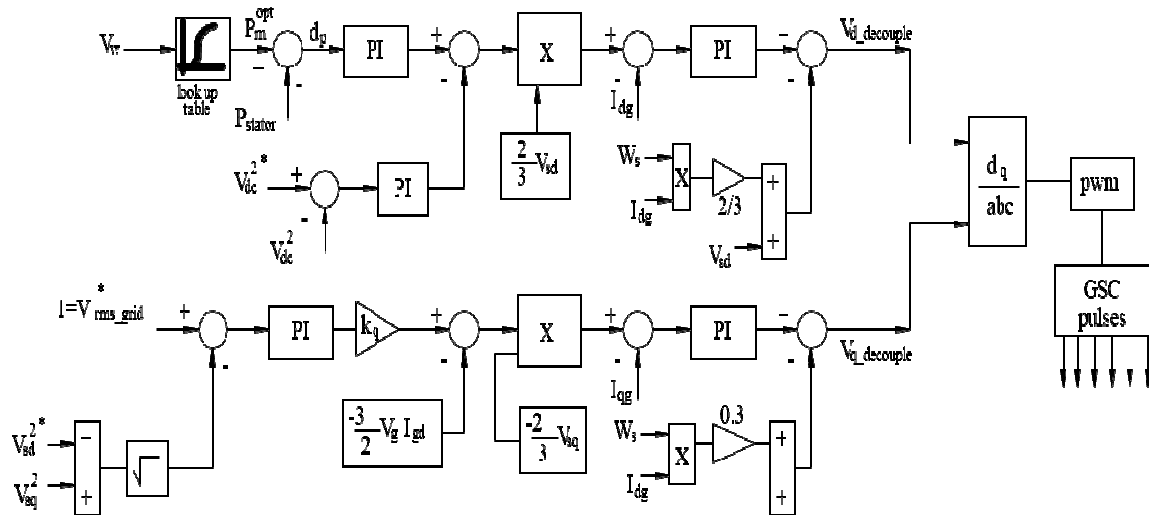

Fig. 1b Grid side controller for DFIG

When dynamic stability has to be improved, proposed technique controls the decrease in stator and rotor flux magnitude and also damps oscillations at the fault instances. To achieve better performance during transients, this paper proposes a strategy for stator frequency reference to change to zero or other value depending type and severity of disturbance. The accurate measurement of stator and rotor parameters like flux, current helps in achieving better performance during transients. The DC offset stator current reduction during transients and making the two axis flux and voltage trajectories circular also improves the efficacy of the system performance during any faults. The equations 8 to 15 help in understanding DFIG

behavior during transient conditions and accuracy of its working depends on measurement of rotor current and flux parameters.

3. Mathematical analysis of RSC and GSC converters for the grid connected DFIG during transient state

A. Three Phase Symmetrical Faults

The stator voltage will reach to zero magnitude during severe three phase's symmetrical fault of low impedance and stator flux Φ_s gets reduced to zero magnitude. The decay in stator and rotor flux is not as rapid as in voltage and can be explained using flux decay theorem. This delay in flux is because of inertia time lagging $\tau_s = \frac{L_s}{R_s}$. This parameter affect the rotor induced emf V_{0r}. The flux during fault is given by

$$\Phi_{sf}^s = \Phi_s^s e^{-t/\tau_s} \tag{8}$$

and $\frac{d\Phi_{sf}^s}{dt}$ is negative, indicating its decay. By substituting (8) in (1b)

$$V_{0r}^s = -\frac{L_m}{L_s}(\frac{1}{\tau_s} + j\omega)\Phi_s^s e^{-t/\tau_s} \tag{9}$$

The above equation is converted into a rotor reference frame and neglecting $\frac{1}{\tau_s}$

$$V_{0r}^s = -\frac{L_m}{L_s}(j\omega)\Phi_s^s e^{-j\omega t} \tag{10}$$

By substituting $\Phi_s^s = \frac{V_s^s}{j\omega_s} e^{-j\omega_s t}$ in (10)

$$V_{0r}^r = -\frac{L_m}{L_s}(1 - s)V_s \tag{11}$$

$|V_{0r}^r|$ is proportional to (1-s)

The converting equation (1a) into the rotor reference frame

$$V_r^r = V_{0r}^r e^{-j\omega t} + R_r i_r^r + \sigma L_r \frac{di_r^r}{dt} \tag{12}$$

The rotor voltage during fault is given by

$$V_r = i_r R_r + \sigma L_r \frac{di_r}{dt} + V_{or} \tag{13A}$$

Or

$$V_r = i_r R_r + \sigma L_r \frac{di_r}{dt} + \frac{L_m}{L_s}\frac{d\phi_s}{dt} \tag{13B}$$

In the above equation (13B), the first two terms on RHS determine the voltage drop by rotor current due to passive elements and the last term determines the EMF induced by the stator flux [17].

During fault, at first instant, Φ_s does not fall instantly described by equation (8). If the machine is running at super synchronous speed with slip (s) near to -0.2pu, during fault, rotor speed, further increases based on the term (1-s) as given by (11). The above speed change is uncontrollable for a generator having higher electrical and mechanical inertia constants. In order to control the rotor current change, V_r^r has to be increased as given by (12). Based on the first reason, a voltage $V_{\Phi s}$ has to be injected in the feed forward path for improving the rotor dip to reach to its near steady state value. Converting equation (10) to synchronous reference frame and considering direct alignment of Φ_{ds} with Φ_s we get,

$$V_{\Phi s} = -\frac{L_m}{L_s}\omega\Phi_{ds} \tag{14}$$

The second technique for voltage increase requirement in a rotor is: dip can be compensated when replacing $s\omega_s$ with $(\omega_{\Phi s} - \omega)$ in cross coupling terms with $s\omega_s L_r' i_{qr}$ and $s\omega_s L_r' i_{dr}$ respectively. The reduction in magnitude and frequency of flux Φ_s, and alignment of flux with the stator voltage without the rate of change in flux angle $\theta_{\Phi s}$ indicates DC offset component in flux.

$$\frac{d\phi_s}{dt} = \omega_{\phi s} = 0 = \omega_f \tag{15}$$

Here, ω_f is the speed of stator flux during fault and this value can be made to zero as offset. The compensation for DFIG during depends on RSC rating. If further decrease in grid voltage, external active devices like energy storage devices or FACTS devices are helpful.

B. Behavior of mechanical and electrical system with the variation in rotor sped and reactive power

The mechanical to electrical relationship is explained as follows. The rotor speed can be expressed as

$$\omega_r = (1-s)\omega_s = p\eta\omega_{\omega t} \tag{16}$$

Where s is slip of DFIG, p is pair of poles of DFIG; η is gearbox ratio and $\omega_{\omega t}$ is wind turbine speed. With the change in wind speed and depending on gears ratio and number of field poles, the rotor speed varies is shown in equation 16. When rotor speed varies, reference quadrature axis current changes, thereby current flow in the rotor circuit varies. The stator output also varies with variation in wind turbine speed and DFIG output power. When slip varies, the voltage in rotor circuit also varies which can be explained as per equations 8 & 9.

The mechanical turbine tip speed ratio (TSR) can be written in terms of radius of turbine wings (R), angular stator speed (ωs), pole pairs and gear box ratio as

$$\lambda = \frac{R\omega_s}{p\eta v_w}(1-s) \tag{17}$$

Increase in stator or grid frequency, TSR increases and vice versa. Similarly with increase in rotor speed or wind speed, TSR decreases and vice versa. Hence when an electrical system gets disturbed, mechanical system also will get some turbulence as electrical to mechanical system is tightly interlinked. The steady state behavior of overall system must satisfy the relation below.

$$\Delta P = \frac{-P_{\omega t}}{(1-s)} - P_{em} = 0 \tag{18}$$

Under normal conditions, the change in turbine output has to be compensated by electrical power output from DFIG. Otherwise slip gets changed and thereby rotor speed changes. Hence imbalance in mechanical to electrical power output ratios, the slip changes. With the change in coefficient of power Cp, the mechanical power varies. The mechanical power changes mostly when wind speed or air density around the turbine wings changes. The electrical power from DFIG changes when mechanical power changes or rotor speed changes or load demand from grid varies.

A considerable decrease in pre-fault steady state voltage V_{0r}^r to certain fault voltage during a three phase fault was explained in above analytics. However, RSC converter is designed to meet V_r^r to match V_{0r}^r for rotor current control and the design has to be made for rating of only 35% of stator rated voltage. The voltage dip during fault can be adopted independently or in coordination by using two techniques is explained below.
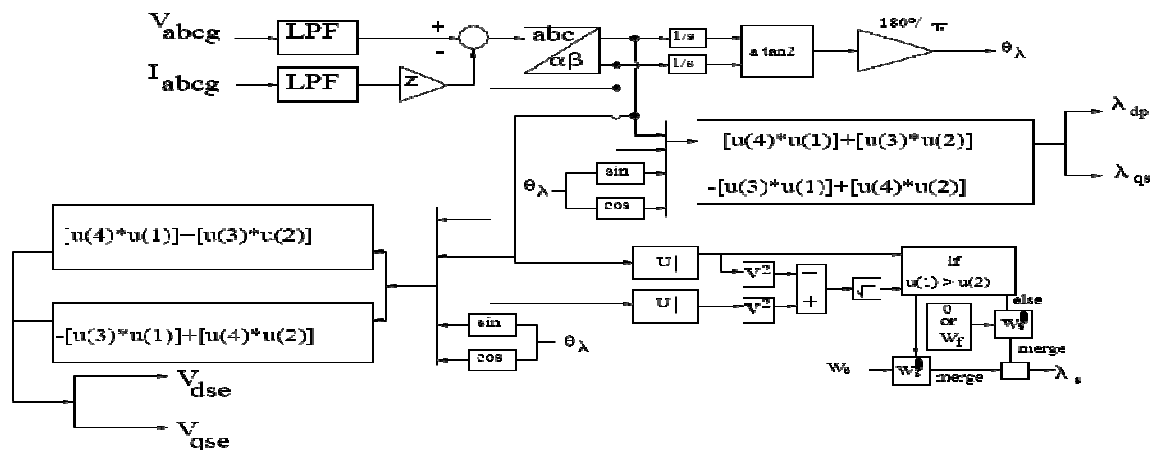

Fig.2. EFOC control loop design with DCOC and rotor flux trajectory control

During fault, at first instant,Φ_s does not fall instantly based on equations (9 or 15). If the machine is running at super synchronous speed with slip (s) near to -0.2pu, during fault, rotor speed further increases based on the term (1-s) as given by (9).The above speed change is uncontrollable for a generator having higher electrical and mechanical inertia constants. In order to control the rotor current change, V_r^r has to be increased. Based on the first reason listed above, a voltage $V_{\Phi s}$ has to be injected in the feed forward path for improving the rotor dip to reach to its near steady state value. The second technique for voltage increase requirement in a rotor is, dip can be compensated by replacing $s\omega_s$ with $(\omega_{\Phi s} - \omega)$ in cross coupling terms $s\omega_s L_r' i_{qr}$ and $s\omega_s L_r' i_{dr}$ respectively. The reduction in magnitude and frequency of flux Φ_s, and alignment of flux with the stator voltage without the rate of change in flux angle $\theta_{\Phi s}$ indicates DC offset component in flux during single line to ground (SLG) fault.

4. Design of IMC for DFIG based system during symmetrical faults

The block diagram representation of the conventional internal model controller (IMC) for DFIG is shown in Fig. 3a. The mathematical modeling of IMC is given below

$$\acute{\omega}_r = \frac{K_t}{J_m} i_q - \frac{B\omega_r}{J_m} - \frac{T_L}{J_m} \qquad (19)$$

$$\acute{\omega}_r^* = \frac{K_t}{J_m} i_q^* - \frac{B\omega_r}{J_m} - \frac{K_t}{J_m} d(t) \qquad (20)$$

$$d(t) = \frac{-T_L}{K_t} - (i_q^* - i_q) \qquad (21)$$

where $\acute{\omega}_r$ is the differential rotor speed of DFIG. The speed controller block CIMC(s) is written as

$$CIMC(s) = G(s) F(s) \qquad (22)$$

$$G(s) = \frac{1}{J's + B^1},$$

Where J' is $\frac{J}{K_t}$ and B' is $\frac{B}{K_t}$

Where G(s) is the internal model block and F(s) is a filter component given by

$$F(s) = \frac{1}{Fs + 1} \qquad (23)$$

where 'F' in the denominator is time constant for filter and 's' is Laplace constant.
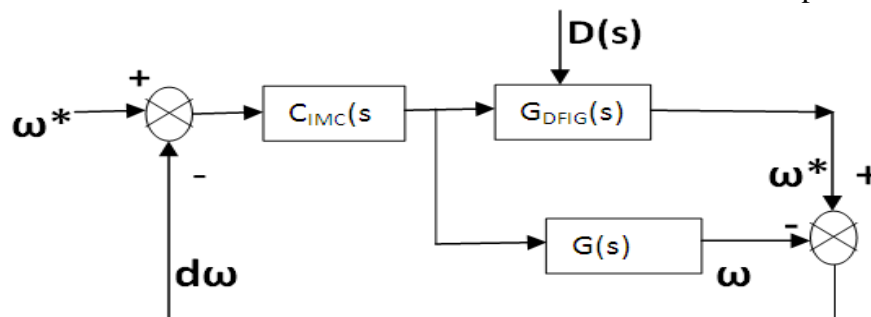

Fig.3a: Conventional IMC technique for DFIG

The improved proposed IMC block diagram is shown in Fig. 3b and its implementation in MATLAB is shown in Fig. 3c.

Fig.3b Improved IMC controller for DFIG

Fig.3c Implementation of IMC controller for DFIG

5. Result Analysis

A. Case 1: with 30% decrease in grid voltage with symmetrical faults at 1s and 2.5s

The performance of EFOC based system with internal model controller (IMC) for recurring faults is shown in Fig. 4 and 5. It is considered in this analysis, a 0.25 seconds three phases to ground fault occurred two times at PCC is considered for the study. A first fault between 1 to 1.25 sec and a second fault between 1.6 and 1.82 s occur at PCC with grid voltage decreasing from 440V to 300V a 30% decrease compared to normal as shown in Fig. 4(i). The decrease in grid voltage during faults depends mainly on location, fault resistance and type of fault. The results of EFOC with PI are available in [17]. The efficacy of the proposed EFOC IMC system can be compared with [3, 10 to 13] for the operation and reactive power control during faults.

The stator and rotor current waveforms are shown in Fig. 4 (ii). The stator current is nearly constant with small deviation at the instants of fault occurring and clearing. The surges at these fault occurring and relieving instants are due to sudden change in capacitor voltage at the back to back converters and also due to sudden inrush of fault current into the stator and rotor windings. The stator current increased from 48A during steady state to 54A during fault and regains to 48A once fault is cleared at both fault instants. There is an increase in rotor current from 46A at steady state to 53A during fault with small increase in frequency.

From the equations (8, 13-17), with the change in stator and rotor flux linkage value and rotor slip, the rotor voltage increases exponentially to certain value. Because of this, based on Fig.2, it can be observed that rotor current thereby stator current will also increase. The surge in torque as shown in Fig. 4 (iii), before fault, the electromagnetic torque (EMT) during fault is to -100Nm. At fault instants at 1s and 1.6s it reached to -100Nm within 1.02s, during fault EMT is again -100Nm. At fault relieving instants 1.25 and 1.85s, EMT is having -280Nm surge and regained to normal very quickly without oscillations. It shows the performance improvement during and after fault and has better working conditions than in available literature. The rotor speed increased from 2190 rpm to 2300rpm at 1s to 1.25s and 1.6s to 1.85s and reaches again 2190rpm after fault clearing.

The change in EMT and rotor speed during fault is shown in Fig. 4(iii). There is a surge in torque at 1s and 2.5s at fault occurring instant. Based on equation (21), moment of inertia J, mechanical torque does not vary, but rotor speed varies. To satisfy the equality constraint with change in rotor speed, EMT also varies. The variation in mechanical torque is low compared to electrical torque because electrical system operates faster than mechanical system as explained by equal area criteria. Due to the inertia in the machine, rotor speed will increase during fault and decreases to normal once fault is cleared. The role of IMC helps in damping out oscillations during fault and to reach steady state quickly. This FC also helps in controlling the flux decay desired by EFOC technique with stubborn control in d and q axis currents in RSC circuit.

The rotor d and q axis current for 30% dip in grid voltage is shown in Fig. 4(iv). These two quadrant currents are -10A and -40A during normal conditions. The peak current values at start for both currents are -20A and 0A. During fault and at the instant of clearance of fault, they are 10 and -100.
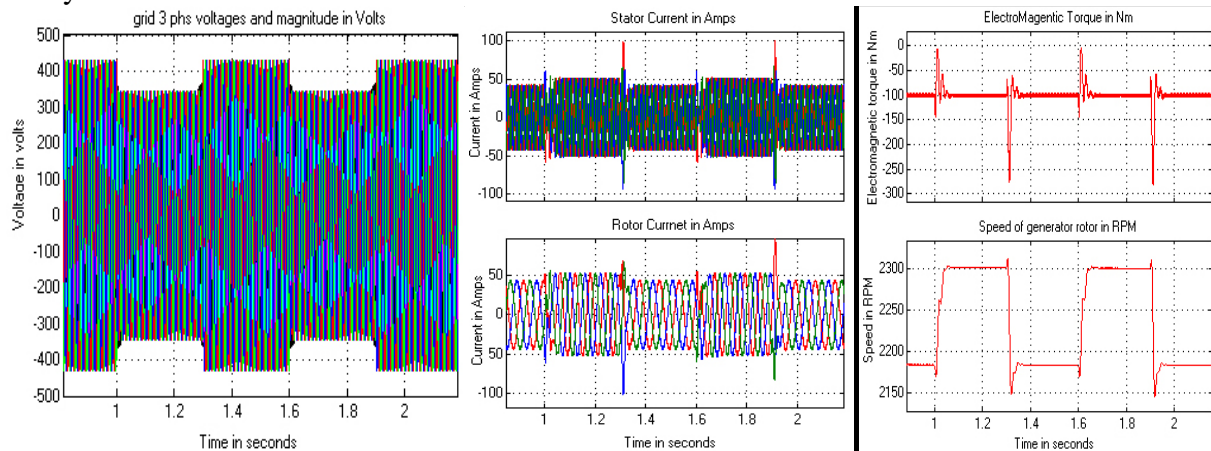
Fig. 4 (i) Grid voltage   Fig. 4 (ii) stator and rotor current
Fig. 4 (iii) EMT and Rotor speed
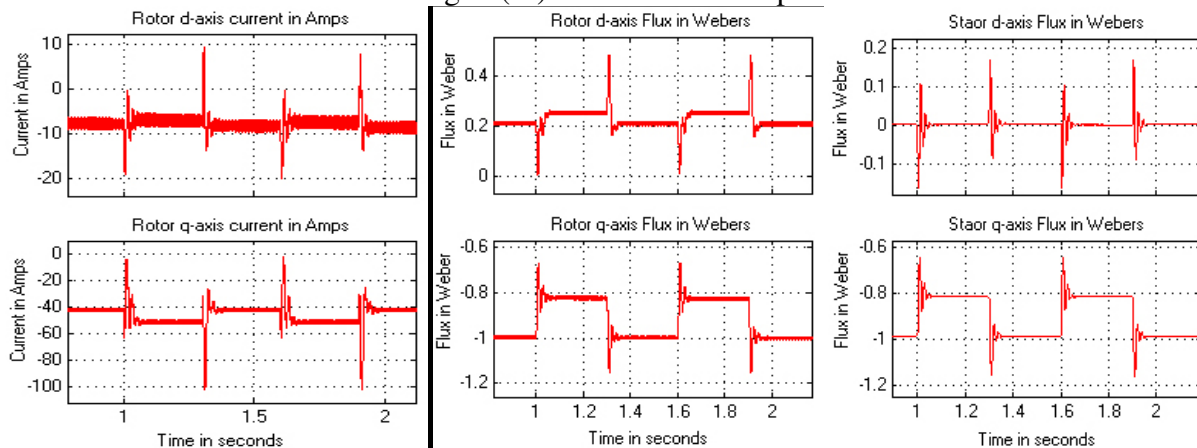
Fig. 4 (iv) d and q axis rotor current in amps   Fig. 4 (v) d and q axis rotor flux in Webbers
Fig. 4 (vi) d and q axis stator flux
Fig. 4 Grid and DFIG parameters variation with 30% grid voltage dip due to symmetrical fault

The d and q axis rotor flux in Weber with 30% dip in grid voltage is shown in Fig. 4(v). The d axis rotor flux is 0.2Wb during normal conditions while, there is an increase to 0.24Wb during both fault instants and regained to normal after the fault is cleared. But q-axis rotor flux magnitude decreased from 1 to 0.8Wb. In the same way, the variation in d and q axis stator flux variations can be understandable from eq. (8) and (9) are shown in Fig. 4(vi). The decay of flux depends on initial stator flux value and stator time constants. The rate of change

414

of stator flux during faults can be controlled without distorting to further level or sampling out oscillations can be possible with EFOC technique as explained by equations 14 and 15. The IMC helps in regulating error and reaching to steady state quickly compared to a PI controller. The EFOC technique with IMC helps in improving stability and minimizing steady state error during and after faults. The stator d axis flux is nearly constant but with surges produced at fault occurrence and relieving instants. The q-axis stator flux changed from -1 to 0.8Wb and d-axis flux remains at 0Wb during 30% dip in grid voltage due to symmetrical fault. The decay in flux is controlled and is maintained without any flux oscillations with EFOC compared to conventional techniques proposed in the literature.

B. Case 2: with 60% decrease in grid voltage with symmetrical faults at 1s and 2.5s

In this case, more severe fault occurred at PCC which makes the grid voltage decrease to 180V from 440 during 1 to 1.25s and 1.6 to 1.85s is shown in Fig.5(i). This decrease in nearly 60% compared to rated voltage without fault. Because of this fault, the stator and rotor current increased to a higher value than previous case with higher impedance fault. But still stator and rotor current are continuous and maintained steady state of 100A during fault as shown in Fig. 5(ii). But at fault instant, stator and rotor current surges are produced with amplitude of 100A and immediately decayed to small value within 0.1sec of fault occurrence for two times. The fault current increased to 100A at 1.1s and maintained uniformly till fault is cleared at 1.25s for the first time fault. The same theory holds good for the second time occurring fault also. When the fault is cleared at 1.25s, a big surge is produced with peak value of 200A can be observed. Later steady state is reached and stator current is maintained to pre-fault state. Its variation is due to sudden change in network impedance and variation in DC voltage across capacitor between converters.

The EMT at fault instants of 1 and 1.6s has a surge value of -200Nm against steady state of -100Nm. It reaches to 0Nm for small duration of 0.05s and attains steady state during fault to -100Nm at 1.1s and 1.7s. When fault was cleared, a severe surge of about -600Nm at this instant is produced as shown in Fig.5 (iii). Immediately after faults are cleared at 1.25s and 1.85sec, EMT is restored. The rotor speed is increased from 2200rpm at both fault occurring instants (1s and 1.6s) to 2900rpm to 0.1s of delay and maintained once fault is cleared at 1.25s and 1.85s. If the fault exists for more than 0.5s time period, the system will sustain to be stable depending on DC capacitance value at back-to-back converters.
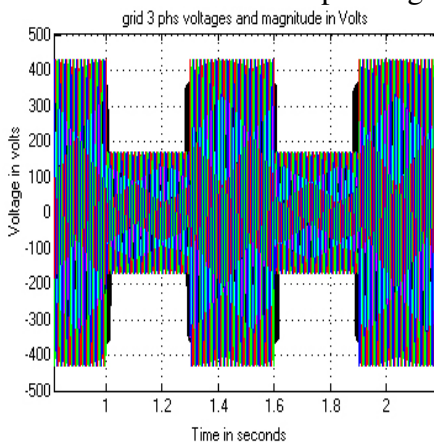

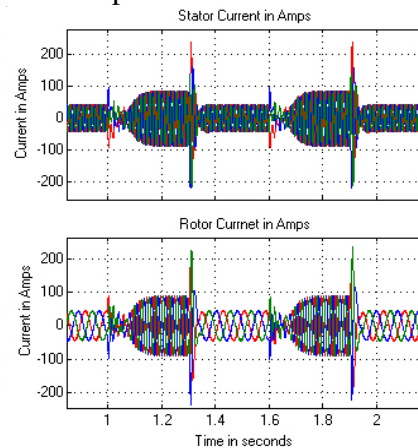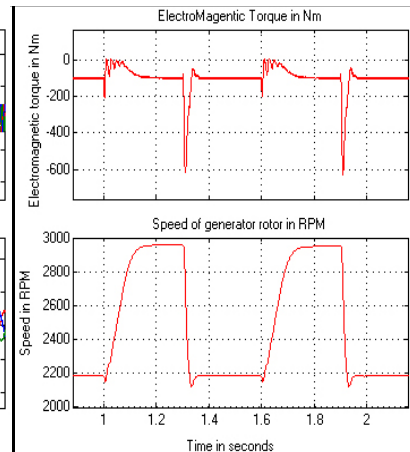Fig. 5 (i) Grid voltage   Fig. 5 (ii) stator and rotor current   Fig. 5 (iii) EMT and Rotor speed
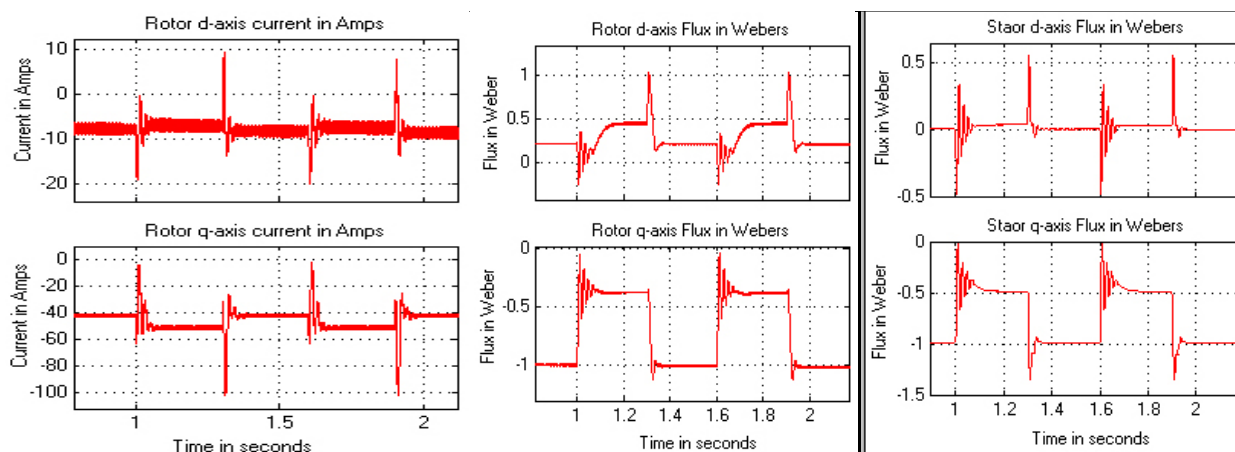
Fig. 5 (iv) d and q axis rotor current in amps   Fig. 5 (v) d and q axis rotor flux in Weber,   Fig. 5 (vi) d and q axis stator flux

Fig. 5 Grid and DFIG parameters variation with 60% grid voltage dip due to symmetrical fault

The rotor d and q axis current for 60% dip in grid voltage is shown in Fig. 5(iv). These currents during steady state are -10A and -40A like previous case. The peak d and q axis current values at fault instants are -20A and 0A. During fault, they are -9 and 55A respectively. At the instant of fault clearance, d and q axis currents produced surges of 10 and -100A and immediately attained pre-fault state.

The d and q axis rotor flux in Weber with 60% dip in grid voltage is shown in Fig. 5 (v). The d axis flux is nearly 0.15Wb during normal conditions, but there is an increase in flux from 0.5Wb during both faults and regained to normal once the fault was cleared. The q-axis rotor flux decreased from 0.9 to 0.4Wb during fault with damped oscillations. The transient can be analyzed from equations (6) and (7), stating with the change in rotor current, the flux will also change. Similarly, the variation in d and q axis stator flux variations can be understandable from equations (8, 9 and 16) as shown in Fig. 5(vi). The decay of flux depends on initial stator flux value and stator time constants.

The rate of change of stator flux during faults are controlled and is limited to further decay is made possible with EFOC technique as explained by equations 15 and 16. The stator d axis flux is nearly constant with sustained oscillations at fault occurrence and relieving instants. These oscillations damped quickly in 0.05s with proposed IMC. If PI is used, they damped in 0.23s and with conventional IMC, it took nearly 0.14s. The q-axis flux changed from -1Wb to -0.5 during 60% dip in grid voltage. The decay in flux is controlled and is maintained without any flux oscillations with EFOC technique and coordination with IMC compared to conventional techniques proposed in the literature.

6. Discussion

A conventional DFIG wind turbine system connected to grid was considered in the analysis with proposed EFOC technique. The system is analyzed for symmetrical recurring voltage sag type grid disturbance and the behavior of DFIG is studied with controllers like IMC. The internal control loops of RSC and GSC with PI are replaced with IMC. Phase grid voltage swell of 30% occurred at 1s and cleared at 1.3s for first time. Another same fault during 1.6 to 1.9s occurs for the second time. Under these two disturbances, generator winding parameters were studied and found that the rotor and stator currents during fault are maintained near its pre-fault value with proposed method. In conventional technique, the waveform will have DC components and harmonics with sub-transient and transient components. The grid voltage increased and current in all phases increased. During sag, voltage in all decreased and current in same phase increased. The stator and rotor winding voltages are nearly constant with EFOC technique with small increase in current is observed.

This performance is however much better than a conventional control techniques like sequence compensation etc.

Table 1: Summary of generator and grid parameters during grid sag and swell asymmetric disturbances

Parameters under study	With 30% dip in grid voltage			With 60% dip in grid voltage		
	Before fault	During fault	After fault	Before fault	During fault	After fault
Grid voltage (pu)	400	340	400	400	180	400
Rotor current (pu)	45	50	45	45	89	50
Stator current (pu)	45	50	45	45	90	45
Rotor speed(rpm)	2180	2300	2180	2180	2990	2180
Electromagnetic torque (pu)	-100	0	-100	-100	0	-150
I_{dr}, I_{qr}	-10, -40	-5, -50	-10, -40	-10, -40	-5,-50	-10, -40
Φ_{dr}, Φ_{qr}	0.2,-1	0.25, -0.8	0.2,-1	0.25,-1	0.5,-0.25	0.25,-1
Φ_{dr}, Φ_{qr}	0,-1	0.1, -0.7	0,-1	0.5,-0.5		0,-1

The proposed EFOC technique helps in controlling the change in affects in other non-faulted phase compared to literature [10, 11, 13-15]. The overall system stability can be improved using EFOC. The deviation in faulty phase generator parameters is controlled and is in limits. The IMC controller is having better performance than with PI controller. The deviation in rotor speed is also lowest with IMC. Compared to PI, PIR is having lesser deviation in speed of rotor. The torque oscillations and their damping are nearly same with PIR and IMC. The magnitude of torque produced for given wind speed, PIR is having more value than with IMC. Compared with proposed EFOC technique and PIR controller in [10, 15], due to symmetrical voltage dip, torque value reached to a smaller value and has oscillations. Stator and rotor currents as well as DC voltage across capacitor are having more harmonic content and waveform distortion in [15] compared to proposed technique.

7. Conclusion

A conventional DFIG wind turbine system connected to grid was considered in the analysis with proposed EFOC technique for recurring fault with internal model controller (IMC) for RSC. A three phase fault is imagined to occur at PCC between 1 and 1.25s and 1.6 to 1.85 seconds making the grid voltage to decrease in 30% and 60%. The rotor and stator currents during fault are maintained near to its pre-fault value with proposed method. In conventional technique, the waveform will have DC components and harmonics with sub-transient and transient components. The stator and rotor winding current increased when severe fault of 60% dip occurred without losing synchronism.

The generator torque during fault is maintained to pre-fault and control in rotor speed can be obtained with proposed EFOC technique with IMC. For faults much greater than 72%, it is found that RSC and GSC controller circuits cannot provide effective compensation in voltage and current, thereby losing synchronism if fault persist for more than 0.3s. It is due to low power rating of RSC and GSC. For conventional technique, EMT has high frequency oscillations with rotor speed uncontrollable during fault. Decay in stator and rotor flux is controlled when changing the reference synchronous speed value as described in Fig. 2 during fault. The above all are the major contributions with the proposed strategy.

Appendix

The parameters of DFIG used in simulation are:
Rated Power = 1.5MW, Rated Voltage = 690V, Stator Resistance Rs = 0.0049pu, rotor Resistance Rr = 0.0049pu, Stator Leakage Inductance Lls = 0.093pu, Rotor Leakage inductance Llr1 = 0.1pu, Inertia constant = 4.54pu, Number of poles = 4, Mutual Inductance Lm = 3.39 pu, DC link Voltage = 415V, Dc link capacitance = 0.2F, Wind speed = 14 m/sec. Grid Voltage = 25 KV, Grid frequency = 60 Hz.Grid side Filter: Rfg = 0.3Ω, Lfg = 0.6nH, Rotor side filter: Rfr = 0.3mΩ, Lfr = 0.6nH.

References

[1] Wang Yun ; Zhao Dong-li ; Zhao Bin ; Xu Hong-hua, "A Review of Research Status on LVRT Technology in Doubly-fed Wind Turbine Generator System", Proc. on ICECE, 2010, pp: 4948 – 4953.

[2] Shuai Xiao ; Hua Geng ; Honglin Zhou ; Geng Yang, "Analysis of the control limit for rotor-side converter of doubly fed induction generator-based wind energy conversion system under various voltage dips", IET Renewable Power Generation, , Volume: 7, 2013 , pp: 71 – 81

[3] Shuai Xiao ; Geng Yang ; Honglin Zhou ; Hua Geng,"An LVRT Control Strategy Based on Flux Linkage Tracking for DFIG-Based WECS",, IEEE Transactions on Industrial Electronics, Volume: 60 , Issue: 7, 2013, pp: 2820 – 2832

[4] Dong liang Xie ; Zhao Xu ; Lihui Yang ; Ostergaard, J. ; Yusheng Xue ; Kit Po Wong, "A Comprehensive LVRT Control Strategy for DFIG Wind Turbines With Enhanced Reactive Power Support", IEEE Transactions on Power Systems, Volume: 28 ,2013 , pp: 3302 – 3310

[5] Lihui Yang ; Zhao Xu ; Ostergaard, J. ; Zhao Yang Dong ; Kit Po Wong, "Advanced Control Strategy of DFIG Wind Turbines for Power System Fault Ride Through," IEEE Transactions on Power Systems, Volume: 27, issue: 2,2012 , Pp: 713 – 722

[6] Rahimi, M. ; Parniani, M., "Efficient control scheme of wind turbines with doubly fed induction generators for low-voltage ride-through capability enhancement", IET Renewable Power Generation, Volume: 4 , Issue: 3,2010, pp: 242 – 252

[7] Jiaqi Liang ; Howard, D.F. ; Restrepo, J.A. ; Harley, R.G., "Feedforward Transient Compensation Control for DFIG Wind Turbines During Both Balanced and Unbalanced Grid Disturbances" IEEE Transactions on Industry Applications, Volume: 49 , Issue: 3, 2013 , pp: 1452 – 1463

[8] Jiaqi Liang ; Wei Qiao ; Harley, R.G., "Feed-Forward Transient Current Control for Low-Voltage Ride-Through Enhancement of DFIG Wind Turbines", IEEE Transactions on Energy Conversion, Volume: 25 , Issue: 3, 2010 , pp: 836 – 843

[9] Vrionis, T.D; Koutiva, X.I. ; Vovos, N.A.,"A Genetic Algorithm-Based Low Voltage Ride-Through Control Strategy for Grid Connected Doubly Fed Induction Wind Generators", IEEE Transactions on Power Systems, volume: 29, 2014 ,pp: 1325 – 1334.

[10] Wenjie Chen, Frede Blaabjerg, Nan Zhu, Min Chen, Dehong Xu, "Comparison of Control Strategies for Doubly Fed Induction Generator under Recurring Grid Faults", ", Proc. on ICECE, 2014, pp: 398 – 404.

[11]Wenjie Chen, Frede Blaabjerg, Nan Zhu, Min Chen, Dehong Xu, "Doubly Fed Induction Generator Based Wind Turbine Systems Subject to Recurring Grid Faults", Proc. on ICECE, 2014, pp: 3097 – 3104.

[12]Wenjie Chen, Frede Blaabjerg, Nan Zhu, Min Chen, Dehong Xu, "Capability of DFIG WTS to Ride through Recurring Asymmetrical Grid Faults", ", Proc. on ICECE, 2014, pp: 1827 – 1834.

[13]Qingjun Huang, Xudong Zou, Donghai Zhu, Yong Kang, "Scaled Current Tracking Control for Doubly Fed Induction Generator to Ride-through Serious Grid Faults", IEEE Transactions on Power Electronics, DOI 10.1109/TPEL.2015.2429153

[14]Wenjie Chen, Dehong Xu, Nan Zhu, Min Chen, Frede Blaabjerg, "Control of Doubly Fed Induction Generator to Ride Through Recurring Grid Faults", IEEE Transactions on Power Electronics, DOI10.1109/TPEL.2015.2443916.

[15]Linyuan Zhou, Jinjun Liu, Sizhan Zhou, "Improved Demagnetization Control of a Doubly-fed Induction Generator under Balanced Grid Fault", IEEE Transactions on Power Electronics, DOI 10.1109/TPEL. 2014.2382603.

[16]Jean Patric da Costa, Humberto Pinheiro, Gunter Arnold, "Robust Controller for DFIGs of Grid-Connected Wind Turbines", IEEE Trans. Ind. Electron , vol. 58, no. 9, pp:4023-4038, Sept. 2011.

[17]Ananth D V N, Nagesh Kumar GV., "Fault ride-through enhancement using an enhanced field oriented control technique for converters of grid connected DFIG and STATCOM for different types of faults", ISA Transactions (2015), http://dx.doi.org/10.1016/j.isatra.2015. 02.014i